Investigation of a Dual Inlet Side Dump Combustor Using Liquid Fuel Injection

F. D. Stull* and R. R. Craig†
Air Force Wright Aeronautical Laboratories, Wright-Patterson Air Force Base, Ohio
G. D. Streby‡
Universal Energy System, Dayton, Ohio
and
S. P. Vanka*
Argonne National Laboratories, Argonne, Illinois

The characteristics of a dual-inlet side-dump combustor configuration suitable for ducted rocket missiles was investigated by injecting a liquid fuel (JP-4) into the two rectangular inlet ducts upstream of the dump plane. Cold flow water tunnel simulations were obtained by injecting small air bubbles into the inlet arms of a plexiglas model and illuminating these by a high intensity slit light source. Combustor performance was obtained by testing a similar stainless steel model on a combustor thrust rig. Combustion efficiency, combustor total pressure loss, lean blow-out limits, combustor pressure oscillations, and surface heating patterns were obtained. A three-dimensional computer code using the k-ϵ turbulence model was used to predict the corresponding cold flowfields with good agreement.

Nomenclature

A	= area
D	= diameter
f/a	= fuel-air ratio
Ht	= dome height
Lc	= combustor length to start of nozzle
P	= pressure; time-averaged pressure
P'	= pressure fluctuation above P
P_t	= stagnation pressure
Sa	= vacuum air specific stream thrust
T_t	= total temperature
Wa	= airflow rate
X	= axial distance
η_c	= combustion efficiency based on thrust
θ	= inlet entry angle

Subscripts

2	= inlet
3	= combustor
5 or ( )$_*$	= nozzle throat

Introduction

CURRENT volume-limited ramjet and ducted-rocket missile designs employ subsonic dump combustors. In such systems, the booster rocket is integrated into the ramjet combustor to conserve missile volume. Such combustors do not contain combustor liners or conventional flameholders within the combustion region and must, therefore, depend to a large extent upon recirculation zones formed by the sudden enlargement area between the inlet duct or ducts and the combustor chamber to act as a flameholder. Previous studies[1-4] have characterized the coaxial dump combustor where a single inlet directs the main airflow into the combustor region in a symmetrical manner. In some applications, a side-dump combustor is employed in which the flow enters the combustion chamber from the side through multiple inlets.[5,6] If a solid fuel containing an oxidizer is used to inject fuel-rich exhaust gases into the head end of the combustor, this engine cycle is known as a solid-fuel gas-generator ramjet or more commonly called a "ducted rocket."

The objectives of the present study are to expand the limited data base on a nonsymmetric configuration of a dual-inlet side-dump combustor and, in particular, to study the effect of varying the distance from the head-end to the inlet arms on head-end vortices which were observed to be important in stabilizing the combustion process.[7] A liquid fuel version of a dual-inlet side-dump combustor was chosen over the ducted rocket version since much more combustor data can be obtained at a lower cost by continually using JP-4 as opposed to a single short run in which a gas generator is consumed and due to local hazard regulations prohibiting fuel containing oxidizers in the airbreathing combustor thrust stand.

Experimental Apparatus

Water Flow Visualization

Water Tunnel Test Facility

The water tunnel test facility is a closed-loop 5.68 m^3/min system that is utilized to simulate the internal cold flow fluid dynamics of ramjet combustor configurations. A clear plexiglas test section allows for complete observation of test combustor flowfields. The water tunnel test facility is capable of testing dual-inlet side-dump combustor configurations over an inlet duct Reynolds number range of 1.3-13 million/m and is instrumented to monitor facility flow conditions for measurements of fluid velocity within the test configuration. Simulations of auxiliary combustor flows such as the gas generation and fuel injectors are also possible. Support systems of the water tunnel test facility include an air/dye injection system and a high intensity light source which can be focused to a narrow plane beam, approximately 3 mm wide. The light source housing can be positioned perpendicular or parallel to the axis of the combustor and moved longitudinally to any point on the combustor axis.

Presented as Paper 83-0420 at the AIAA 21st Aerospace Sciences Meeting, Reno, Nev., Jan. 10-13, 1983; received Aug. 8, 1983; revision received Sept. 9, 1984. This paper is declared a work of the U.S. Government and therefore is in the public domain.

*Supervisory Aerospace Engineer. Associate Fellow AIAA.
†Aerospace Engineer.
‡Test Engineer. Member AIAA.
§Engineer.

Water Tunnel Combustor Model

The dual-inlet side-dump combustor consists of two rectangular inlet ducts, a combustor, a nozzle, and a gas generator section. The test model configuration and physical dimensions are shown in Fig. 1.

The two rectangular inlet ducts intersect the combustor at an inlet angle θ of 45 deg. The centerline of both inlet ducts intersect the combustor at the same axial station and are located radially at 90 deg to each other. The internal dimensions of the inlet ducts are 5×7 cm. The upstream edge of the inlet ducts is taken as the combustor longitudinal zero reference point. Longitudinal measurements downstream of the zero reference point are positive.

The combustor is a 15.2 cm diam. plexiglas pipe and measures 99 cm in length from the combustor longitudinal zero reference point to the exit nozzle. The combustor dome plate is located at the upstream end of the combustor and can be positioned axially from the zero reference point to approximately 25 cm forward of the inlet ducts. Test results reported in this paper are limited to a flat dome plate with no gas generator fluid flow. The exit of the combustor is flanged so that different exit area nozzles can be used. Nozzle area ratios, A^*/A_3, of 0.20, 0.29, and 0.39 are available with $A^*/A_3 = 0.29$ being selected for these tests.

Combustion Tests

Combustor Thrust Facility

The combustor thrust rig consists of a thrust stand designed for measuring absolute values of thrust and a Mod Comp II computer-controlled data acquisition system. The movable deck of the thrust stand is 4.27 m long and 1.2 m wide. The deck is suspended from four flexures 38.1 cm long, 15.2 cm wide, and 1 mm thick. Periodic calibration of the thrust stand is accomplished by applying a force at the combustor centerline through a reference load cell which is capable of indicating force up to 9000 N in tension or compression. Additional calibration is accomplished prior to each combustor test run.

High pressure air is supplied from 2×10^6 N/m^2 compressors through twelve 5 cm diam flex hoses to a J-85 combustor preheater mounted on the thrust stand. Makeup oxygen is added considerably upstream of the preheater. Inlet air temperature is measured with three shielded chrome/alumel thermocouples located downstream of the preheater.

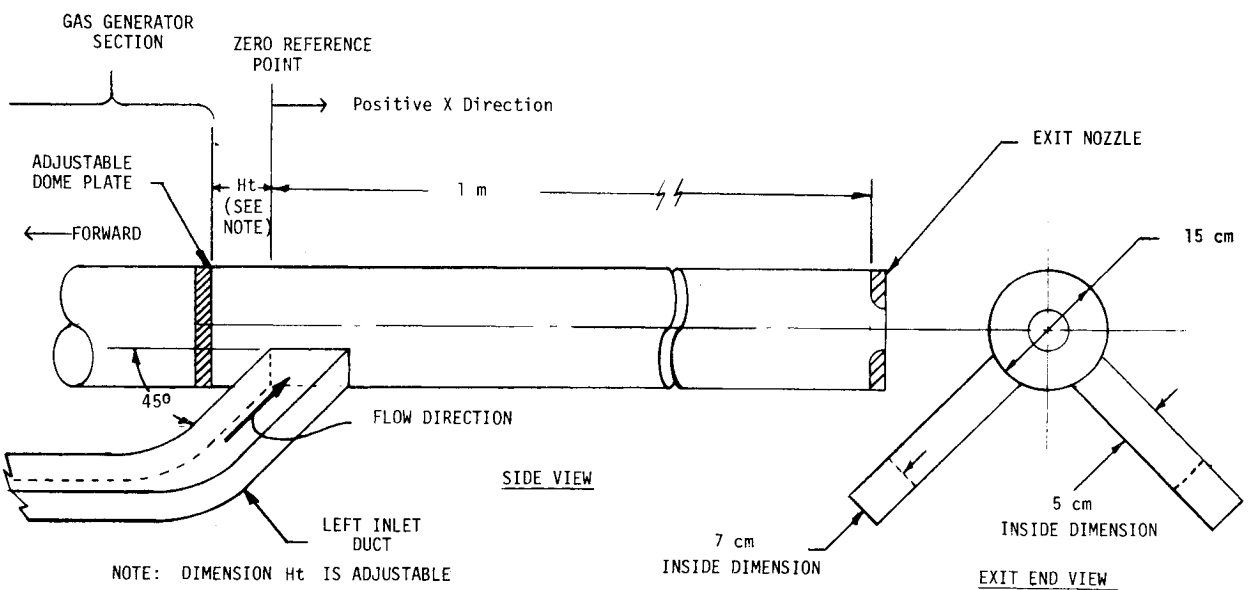

Fig. 1 Water tunnel combustor configuration.

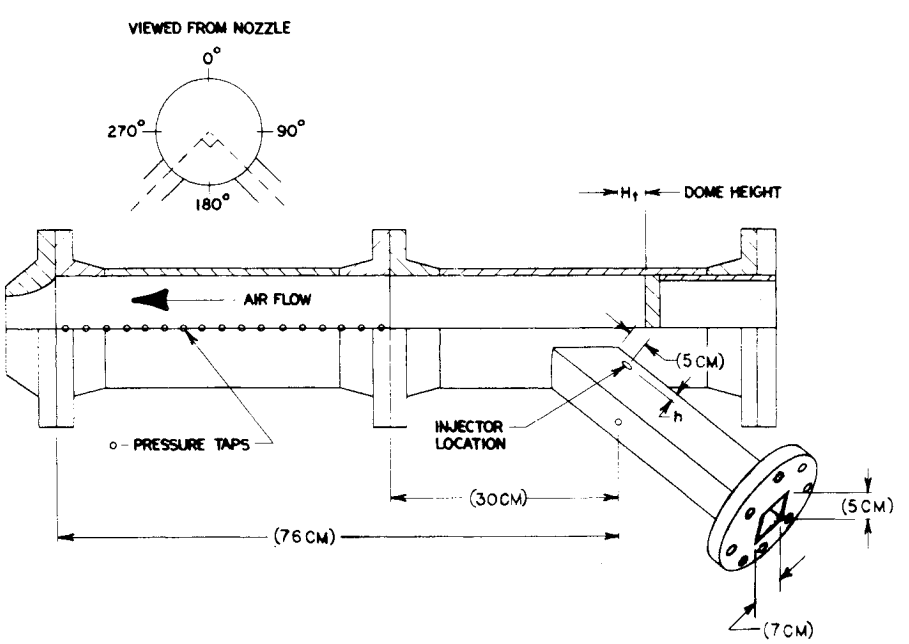

Fig. 2 Combustor test hardware.

Air mass flow is measured using flange tap, square edge orifice plates; oxygen flow rates by a vortex shedding flowmeter; and fuel flow rates by turbine type flowmeters. The nozzle of the test model is connected to the laboratory exhaust system by means of a simple labyrinth seal to maintain exhaust pressures low enough to ensure a choked exit nozzle for all combustion tests.

Combustion Test Hardware

A schematic of the combustor hardware is shown in Fig. 2, and is similar to the water tunnel hardware except that it was fabricated from stainless steel pipe. Three sets of inlet-combustor sections were fabricated with the inlet flow intersecting the combustor axis at $\theta = 30$, 45, and 60 deg. The dome region of the combustor was constructed with spacers which allowed its depth to be varied from $Ht = 2.54$ to 15.2 cm from the upstream intersection of the inlet arm with the combustor. Each inlet arm was 5×7 cm and included a 2.77×4.67 cm choke plate at the beginning of the two-dimensional arm to assure equal flow through each arm.

Fuel injection struts were simple heavy wall 6-mm tubing with the ends welded shut and simple orifice patterns drilled in the side walls. The centerline of each fuel strut was located 5 cm from the combustor outer wall, on the upper surface of each inlet arm, parallel to the centerline of the inlet arm. The distance from the most upstream outer wall, perpendicular to the centerline of the inlet arm varied from 1 to 1.4 to 2.4 cm for the 30-, 45- and 60-deg arm, respectively. The tubes were inserted perpendicular to the inlet arm centerline and parallel to the most upstream inner wall. Only one fuel tube was used in each arm, but the number of orifices in each tube could be varied from two to four and the direction of fuel spray was varied from 90 deg to the flow to parallel with the flow.

Three water-cooled sonic nozles, 7.6 cm in length from the start of the nozzle to the sonic point, were available with area ratios of 0.4, 0.5, and 0.6. Water-cooled nozzles were used in order to limit the variation in A^* during a run as this quantity is used in calculating the combustor performance. All combustion efficiency results given in this paper are computed from thrust measurements by the procedure described in Ref. 1.

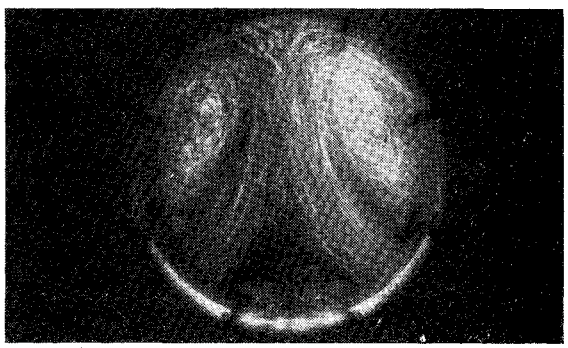

a) Axial position at 10 cm.

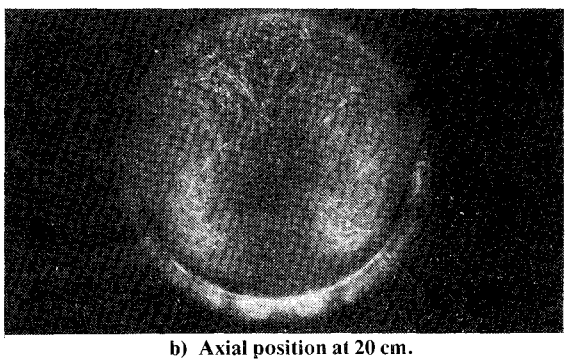

b) Axial position at 20 cm.

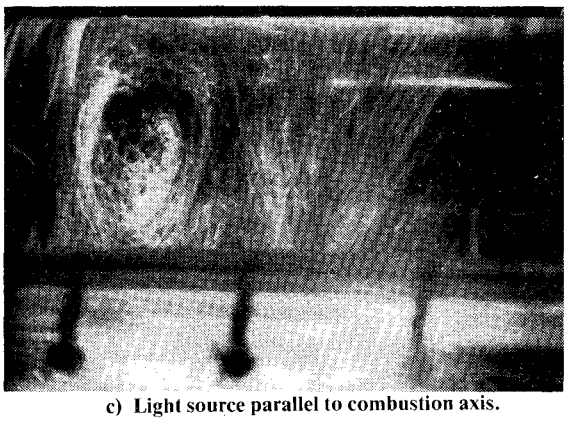

c) Light source parallel to combustion axis.

Fig. 3 Photographs of baseline combustor streamline patterns.

Results and Discussion

Water Flow Visualization Tests

Baseline Configuration

The baseline configuration selected had 45-deg inlet ducts, a 5-cm dome height, and a nozzle area ratio, $A^*/A_3 = 0.29$. Water flow was balanced in the inlet ducts at a constant flow velocity of 2.67 m/s corresponding to an inlet duct Reynolds number of 1.8×10^5. Photographs (0.25-s shutter speed) showing the time-mean streamline patterns produced by the air bubbles are shown in Figs. 3a and 3b for two axial stations downstream of the leading edge of the air inlet duct. Figure 3c shows the corresponding flow, but includes the dome region, when the light source was aligned parallel to the axis of the combustor. Detailed sketches of cross-sectional flow patterns made from visual observations are shown in Fig. 4. Examination of such photographs, sketches, and motion pictures reveals the flow processes. The general nature of the flow appears to consists of two primary zones: 1) a recirculating flow in the dome region of the combustor which can be bistable; and 2) two counterrotating helical vortices trailing

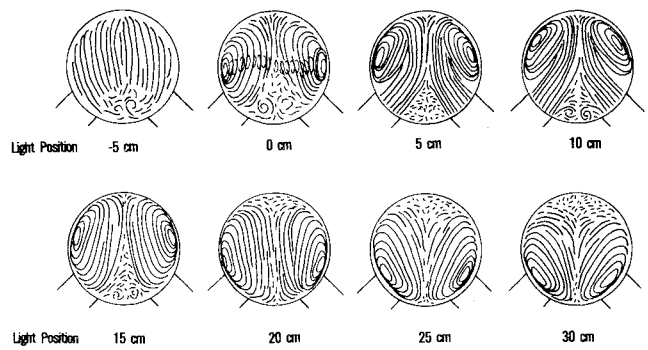

Fig. 4 Sketches of baseline combustor streamline patterns.

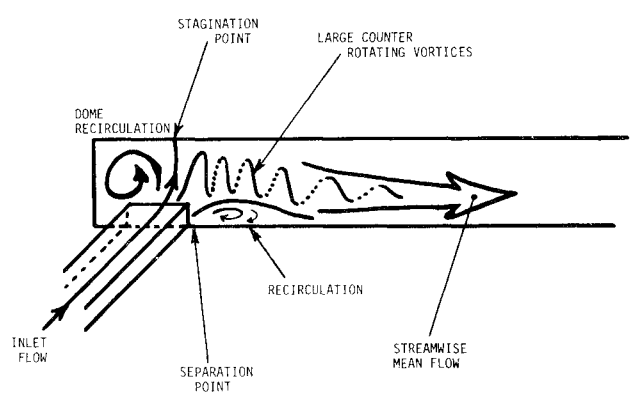

Fig. 5 Major combustor flow regions.

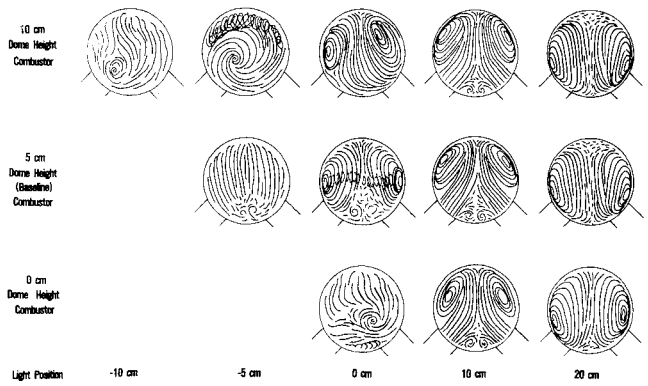

Fig. 6 Effect of dome height on streamline patterns.

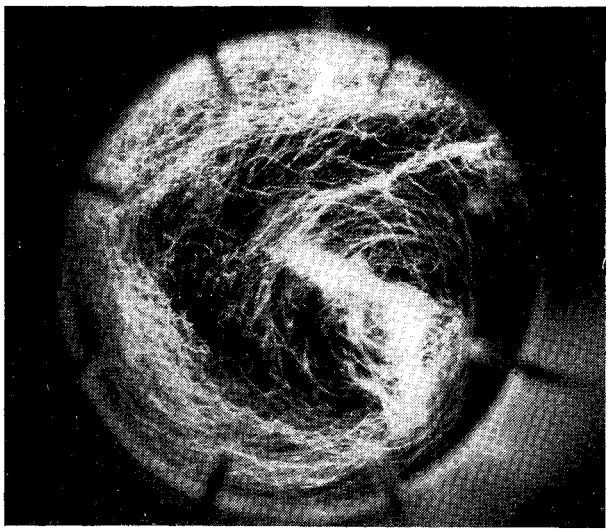

Fig. 7 Photograph of 10-cm dome height combustor at $x = -5$ cm.

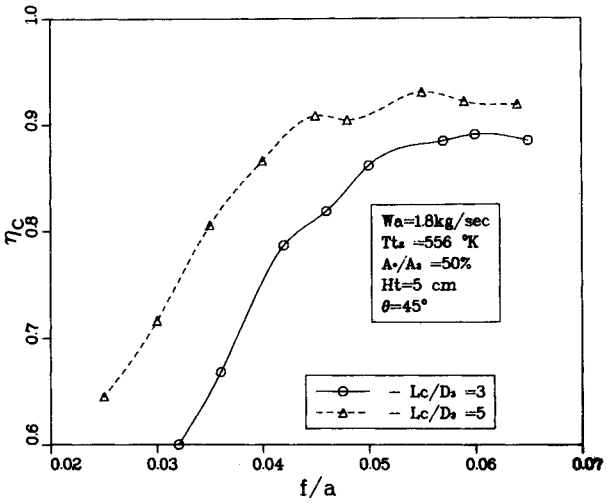

Fig. 8 Effect of combustor length to diameter ratio.

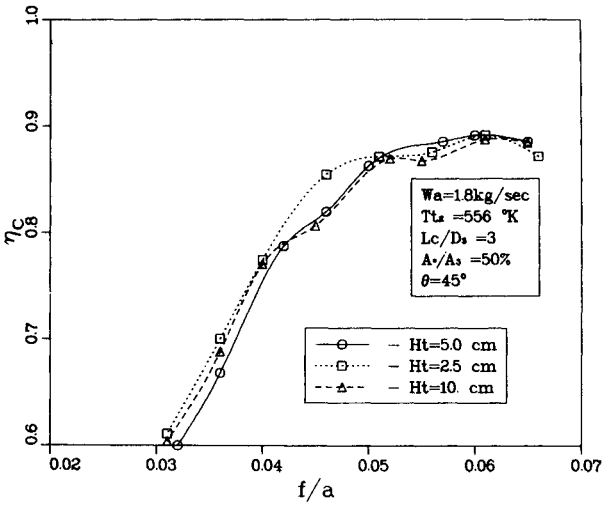

Fig. 9 Effect of dome height.

in the streamwise direction from the inlet. In addition to these, there are several other secondary flow zones which include a pair of small counterrotating vortices immediately downstream of the inlet on the bottom side of the combustor. This recirculation region is the result of flow separation due to the inlet flow configuration. Figure 5 illustrates these major combustor flow regions.

Effect of Dome Height

The effect of varying dome height on the overall flowfield at selected axial stations is shown in Fig. 6 for $Ht = 0$ and 10 cm in addition to the baseline. Although the character of the flow in the dome region is drastically changed by varying dome height, the overall flowfield pattern downstream of the air inlet duct is relatively unaffected. Figure 7 is a photograph of the flow within the dome region for the $Ht = 10$ cm combustor showing the vortex formation at the -5 cm axial station.

Combustion Tests

Baseline Combustor

The baseline combustor was selected to correspond closely to the water flow visualization combustor with $\theta = 45$ deg, $Ht = 5$ cm, and $A^*/A_3 = 0.50$. However, instead of choosing $Lc/D = 5$ for the baseline, $Lc/D = 3$ was chosen in order for combustor performance to be more sensitive to configuration changes. Over a dozen initial tests were made to optimize the fuel injection pattern. These tests consisted of variations in the injection angle relative to the airflow, symmetry of the orifice location relative to the inlet arm walls and number of orifices per injector. Differences in performance due to these changes were relatively minor with the two-orifice injector; injection perpendicular to the airstream gives the best performance over the entire fuel-air ratio range. This injector configuration was then adopted for all remaining combustion tests. Baseline operating conditions were $T_{t2} = 555$ K and an airflow rate of 1.8 kg/s, which resulted in a mean combustor pressure of 2.28×10^5 N/m^2. Combustion efficiency vs fuel-air ratio is shown in Fig. 8 for the baseline combustor as well as for the $Lc/D = 5$ configuration. These data are uncorrected for heat loss; hence, the actual combustion efficiency would be about 3-5% higher than the values shown.

Effect of Dome Height

The effect of dome height on combustion efficiency is shown in Fig. 9 where Ht was varied from 2.54 to 10 cm. Very little difference in η_c is noted except for one isolated data point for $Ht = 2.54$ cm at a fuel-air ratio of 0.046. This insensitivity to dome height is apparently due to the relatively strong recirculation zone at the combustor head-end which is independent of the range of Ht tested. This postulate is further reinforced by the observed greater sensitivity of the 60-deg inlet arm performance to dome height.

Effect of Inlet Entry Angle

The effect of inlet arm angle on combustion efficiency is shown in Fig. 10 for $\theta = 45$, 30, and 60 deg. Although larger

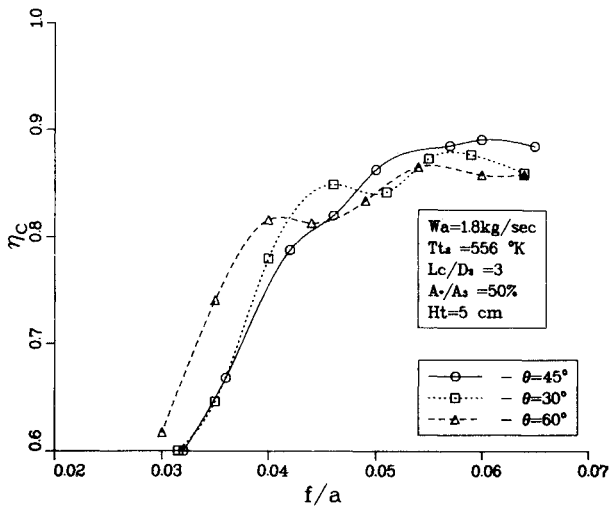

Fig. 10 Effect of inlet angle on combustion efficiency.

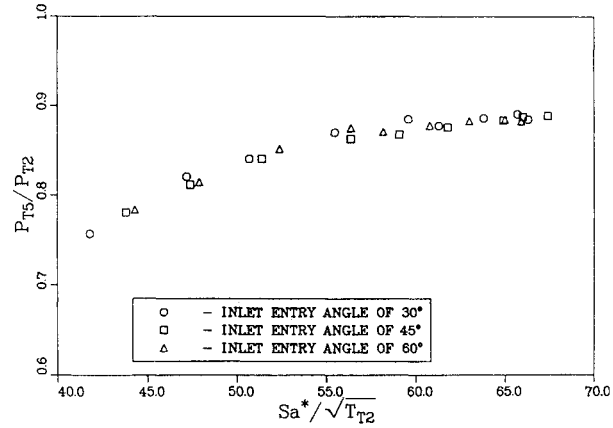

Fig. 11 Effect of inlet entry angle on combustor total pressure ratio.

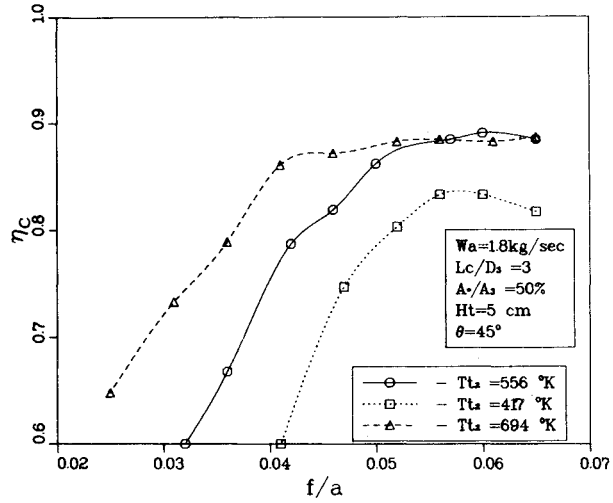

Fig. 12 Effect of inlet air temperature.

deficiencies in η_c are noted than for changes in dome height, these changes are still relatively minor, except at f/a less than about 0.04 where $\theta = 60$ deg clearly exhibits the best performance. As mentioned previously, the 60-deg inlet arm angle was more sensitive to combustor dome height. Figure 11 gives the corresponding combustor total pressure recovery results for these tests. As can be seen, varying θ had little effect on overall combustor performance, even for a relatively short combustor ($Lc/D_3 = 3$). This is in general agreement with the water tunnel cold flow mixing results in which the flowfield 45.7 cm downstream of the combustor was nearly identical for all configurations tested.

Effect of Inlet Air Temperature

Although changes in inlet air temperature have no counterpart in water tunnel simulation, T_{t2} can have a significant effect on combustion efficiency, particularly at the lower fuel-air ratio as seen in Fig. 12. Similar results are found with the $Lc/D_3 = 5$ combustor with the main difference being the fuel-air ratio at which the different temperature curves begin to merge. For $Lc/D_3 = 3$, only the efficiency curves for 694 and 555 K merge at a fuel-air ratio greater than 0.055. At $Lc/D_3 = 5$, the 694 and 555 K efficiency curves merge above a fuel-air ratio of 0.035, and above 0.045 the 416 K efficiency curve merges with the other two temperature curves.

Combustor Pressure Oscillations

Previous small-scale ramjet combustors have experienced both low- and high-frequency combustion oscillations.[4,8] Large-amplitude, low-frequency acoustic oscillations are particularly detrimental to ramjet engines since they can interact with the inlet and reduce the available pressure margin. High-frequency oscillations, while capable of increasing combustion efficiency due to enhanced turbulence mixing, can be detrimental to the thermal protection system due to increased heat transfer and vibration loads. As a result, a close-coupled, high-frequency response Kistler pressure transducer was attached to the front combustor flange to detect any pressure oscillations occurring during all combustor tests. The combustor was found to be extremely oscillation-free. High-amplitude (P'/P_3 greater than 10%) low-frequency oscillations with the baseline combustion occurred only at inlet air temperatures below 458 K as shown in Fig. 13.

General observations obtained from many combustion tests conducted with the dual-inlet side dump combustor are now sumarized. The amplitude of the instabilities increased for the following variables: decreased air temperature; decreased combustor length; increased fuel-air ratios, lower inlet entry angles, and increased nozzle throat size. The frequency range of the observed oscillations was in the 100-325 Hz range and was observed to increase with the following variables: increased air temperature, decreased combustor length, lower inlet entry angles, and increased nozzle throat size. The observed frequencies, pressure phase angles, and amplitude variations caused by configuration and flow property changes, generally agree with the changes that would be predicted for an entropy wave-type instability cycle.[9]

Surface Heating Patterns

Using bare wall stainless steel combustor hardware instead of water-cooled combustors allows one to obtain additional information about what is happening within the combustor flowfield. This is shown in Fig. 14 where photographs were taken of the hot combustor. As seen earlier from the water tunnel flow visualization results, the side-dump air entries into the combustor produce large vortical flow patterns which can produce very nonuniform heating patterns along the combustor walls. Maximum heating appears to occur near the top of the combustor upstream of the air entry stagnation point due to the strong dome recirculation pattern, and near the bottom of the combustor immediately downstream of the inlet due to the pair of small counterrotating vortices.

Combustor Modeling

The cold flow patterns obtained in the water tunnel were investigated by a modified version of the FLOW3D code.[10] Computations were performed for dome heights of 5 and 0 cm and for injection angles of 45 and 60 deg. The flowfields

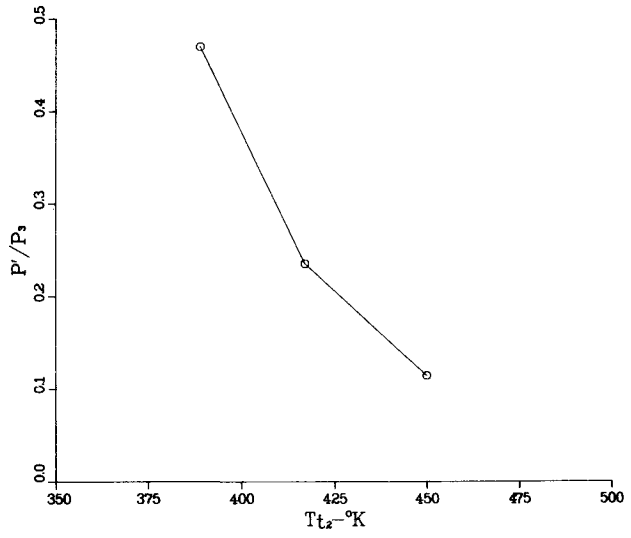

Fig. 13 Effect of inlet air temperature on combustor pressure oscillations.

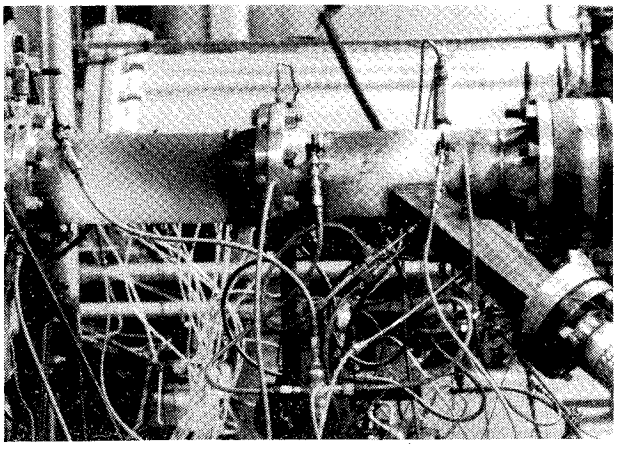

Fig. 14 Combustor heating pattern.

were obtained by solving the steady-state mean flow equations along with a two-equation (k-ϵ) model of turbulence. Because of limitations on space, only the baseline-computed flowfield is shown here. A complete set of results has been documented in a separate paper.[11] All results have been generated with a finite-difference grid of 3500-4000 nodes (11×10 nodes in cross section).

Figure 15 shows the computed flowfield for the baseline case. The flow patterns agree well with flow visualization tests, except in the dome region. Since the dome region is periodic and bistable under certain conditions, the present calculations which solve the steady-flow equations are not expected to give good agreement with the data in this region. The flowfield downstream of the inlet is, however, well characterized by the computations.

Conclusions

The cold flowfield of a dual-inlet side-dump combustor has been well documented by water tunnel results providing insight into the mixing-controlled processes of this combustor. Variations in dome height (Ht) greatly affect the head-end flowfield, but have little influence on the flowfield downstream of the inlet entry ducts.

Combustion tests using liquid fuel injection into the inlet air ducts show that excellent combustor performance can be obtained in a 15.2 cm diam dual-inlet side-dump combustor configuration suitable for ducted rocket missiles. Combustor performance was not sensitive to variations in dome height and only mildly affected by inlet entry angle (θ).

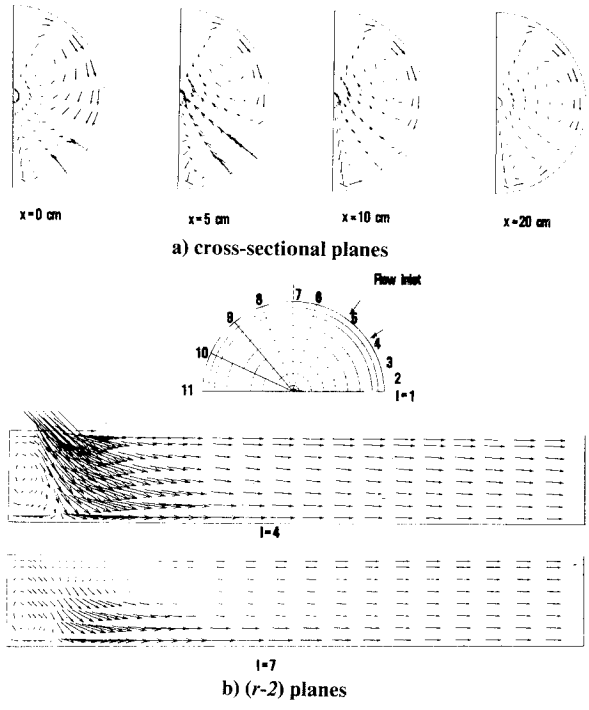

Fig. 15 Computed flowfield patterns for baseline combustor (Ht = 5 cm and θ = 45 deg).

Combustor pressure oscillations were not a problem for this combustor configuration, except at inlet air temperatures below 458 K.

Surface heating patterns obtained by using bare wall combustors nicely supplement the water tunnel flow visualization results and can be of value in locating hot spots for the development of reliable ramburner thermal protection systems.

A three-dimensional, steady-state isothermal computer code using the standard two-equation (k-ϵ) turbulence model gave good agreement with the water tunnel flow visualization results, except in the dome region where the flow was periodic and bistable under certain conditions.

References

[1] Stull, F. D., Craig, R. R., and Hojnacki, J. T., "Dump Combustor Parametric Investigations," *ASME Fluid Mechanics of Combustion, Joint Fluids Engineering and CSME Conference,* May 1974, pp. 135-152.

[2] Stull, F. D. and Craig, R. R., "Investigation of Dump Combustors with Flameholders," AIAA Paper 75-165, Jan. 1975.

[3] Craig, R. R., Buckley, P. L., and Stull, F. D., "Large Scale Low Pressure Dump Combustor Performance," AIAA Paper 75-1303, Oct. 1975.

[4] Craig, R. R., Drewry, J. E., and Stull, F. D., "Coaxial Dump Combustor Investigations," AIAA Paper 78-1107, July 1978.

[5] Boray, R. S. and Chang, C., "Flowfield Studies of Dump Combustors," *Fifth International Symposium on Airbreathing Engines,* Feb. 1981, pp. 22-1-22-8.

[6] Krohn, E. O. and Triesch, K., "Multiple Intakes for Ramrockets," *AGARD Conference Proceedings No. 307,* Oct. 1981, pp. 12-12—12-14.

[7] Choudhury, P. R., "Characteristics of a Side Dump Gas Generator Ramjet," AIAA Paper 82-1258, June 1982.

[8] Clark, W. H., "An Experimental Investigation of Pressure Oscillations in a Side Dump Ramjet Combustor," AIAA Paper 80-1117, June, 1980.

[9] Keklak, J. A., "A Low-Frequency Instability Mechanism in a Coaxial Dump Combustor," MS Thesis, Massachusetts Institute of Technology, Cambridge, Mass., Jan. 1982.

[10] Vanka, S. P. "FLOW3D: A Computer Program for Modelling Three-Dimensional Recirculating Turbulent Flows and Heat Transfer," Argonne National Laboratory, Argonne, Ill., Rept. ANL-83-86, 1983.

[11] Vanka, S. P., Stull, F. D., and Craig, R. R., "Analytical Characterization of Flowfields in Side Inlet Dump Combustors," AIAA Paper 83-1399, June 1983.